TECHNIQUE FOR RECONSTRUCTING THE OZONE PROFILES FROM UV LIDAR DATA: CORRECTION FOR AEROSOL AND TEMPERATURE STRATIFICATION

V.V. Zuev, M.Yu. Kataev, and V.N. Marichev

Institute of Atmospheric Optics,
Siberian Branch of the Russian Academy of Sciences, Tomsk
Received July 6, 1997

We consider a technique of reconstructing the ozone profiles from lidar data that allows for aerosol and temperature stratifications in the stratosphere. The technique is incorporated into a new version of the SOUND software package. The modeling results presented clearly show the necessity of taking into account the aerosol and temperature stratifications. We also present here some results of the package application to reconstructing real ozone profiles. It is shown that the application of the developed technique makes it possible to reduce the errors in reconstructing the ozone profile to 20–30% *owing to the use of the data on the aerosol and temperature stratifications.*

The differential absorption lidars[1] are widely used for sensing of atmospheric ozone. Both the lidar instrumentation and measuring methods are being permanently developed and improved. This fact makes it possible to increase the sensing range, spatial resolution and measurement accuracy. The techniques for data processing also are being developed. Let us note that the tendency to increase the measurement accuracy makes one to include into the processing procedure not only new mathematical algorithms but also to take into account some physical peculiarities characteristic of the problem. In this paper we consider the problem of reconstruction of the spatial distribution (the profile) of stratospheric ozone taking into account the stratifications of different interfering factors, among which we place special value on aerosol and temperature.

The lidar complexes for studying the ozone in the stratosphere become the main instrument in the international network for observing stratospheric changes.[2] As a rule, Xe–Cl excimer lasers emitting at 308 nm wavelength within the Huggins ozone absorption band[3,4] are used in such lidars. Due to significant width of the band (210–340 nm), the second reference wavelength should be distant from the basic one to more than 20–30 nm to the side of its increase, in order to obtain a sufficient value of the differential absorption coefficient. This specific feature of operation with a wide absorption band and significant difference between the wavelengths causes the following peculiarities which significantly differ from operation with an isolated absorption line (or a narrow absorption band): a) there are no special requirements to the spectral characteristics of laser radiation, because within the limits of the Xe–Cl laser spectrum width (< 1 nm)[3,5–6] the absorption band spectrum remains practically constant; b) a difference in aerosol scattering, which should be corrected for, appears due to a significant difference between the wavelengths.

Let us also note that it is necessary to correct the ozone absorption coefficient values when calculating the ozone profile, due to the temperature dependence of the absorption by ozone.[7] We suggest to use for this purpose the temperature and aerosol stratifications reconstructed at the reference wavelength. It is also necessary to take into account the interference of absorption of other gases which introduce uncertainty into the reconstructed ozone profiles. Let us consider in details the questions related to estimation and correction for the effect of aerosol scattering and temperature dependence of the absorption spectrum and absorption of the interfering gases on the accuracy of reconstruction of the ozone concentration profiles.

CORRECTION FOR THE AEROSOL SCATTERING

When sensing the tropospheric ozone, where the lidar signals due to aerosol scattering prevail over the molecular scattering signals, the problem of correct determination of the aerosol scattering coefficient is especially urgent. As a rule, the Klett method or its modifications[8–11] are used for these purposes. This method makes it possible to reconstruct the ozone concentration profiles in the troposphere by the differential absorption technique. However, such an approach has some disadvantages related to the choice of the initial parameters, that finally results in a noticeable error in reconstructing the aerosol scattering coefficients from real signals. The situation can become more difficult because the parameters may vary along

0235-6880/97/09 691-06 $02.00

the sensing path and significantly differ from the average values over the path as a whole. When sensing ozone in the stratosphere, there is a possibility to avoid the disadvantages related to the use of the Klett method.

Let us consider the expression for determining the ozone concentration, writing it in the integral form (in terms of optical thicknesses):

$$\tau_{O_3}(h) = \frac{1}{2} \ln \frac{N_{\lambda_2}(h)}{N_{\lambda_1}(h)} - \frac{1}{2} \ln \frac{\beta_{\lambda_1}(h)}{\beta_{\lambda_2}(h)} - \Delta\tau_a(h) -$$

$$- \Delta\tau_m(h) - \Delta\tau_g(h), \qquad (1)$$

where τ_{O_3} is the ozone optical thickness, $\Delta\tau(h) = \tau_{\lambda_1}(h) - \tau_{\lambda_2}(h)$ is the difference between the optical thicknesses caused by the aerosol and molecular scattering, as well as by the absorption by other gases.

If one does not take into account four last terms in Eq. (1), this results in the errors in determining the ozone concentration profile, because these values make a sufficient contribution into the ozone optical thickness. Correction for the molecular scattering $\Delta\tau_m$ is calculated quite exactly by using the atmospheric models (see, for example, Ref. 12). Correction for the aerosol extinction $\Delta\tau_a$ in the stratosphere at the background aerosol concentrations is not significant, because in these spectral and altitude ranges molecular scattering prevails over the aerosol one. The aerosol content in the stratosphere can increase by one order of magnitude or more after the volcanic eruptions, that makes the aerosol and molecular thicknesses comparable in value. For example, after Mt. Pinatubo eruption (1991) the maximum aerosol content in the stratosphere over Tomsk was observed in January and February 1992.[12] The measured values of the background and peak values of the integral backscattering coefficient $B_\pi = \int_{15\ km}^{30\ km} \beta_\pi(h)\, dh$ at the wavelength of 532 nm were $1 \cdot 10^{-4}$ and $3 \cdot 10^{-3}$ sr^{-1}, respectively. Recalculating to the wavelengths $\lambda_1 = 308$ and 353 nm using the data from the mean cyclic model of the aerosol atmosphere,[13] we obtained the aerosol thicknesses for the background conditions $\tau_a(\lambda_1) = 0.0065$; $\tau_a(\lambda_2) = 0.006$ and for the volcanic emissions $\tau_a(\lambda_1) = 0.022$; $\tau_a(\lambda_2) = 0.02$. The difference between the aerosol optical thicknesses in the first case was 0.0005, and in the second case 0.002. The ozone optical thickness in the same altitude range was ≈ 0.4. It is seen that the contribution of the aerosol correction does not exceed 1% of the ozone optical thickness. The weak effect of the aerosol thickness can be explained by its weak spectral dependence in the wavelength range 300–350 nm.

To calculate the contribution coming from the elastic backscatter let us write the expression for the ratio of the backscattering coefficients in the form

$$\frac{\beta_\pi^{\lambda_1}}{\beta_\pi^{\lambda_2}} = \frac{\mu\, \beta_a^{\lambda_2} + \psi\, \beta_m^{\lambda_2}}{\beta_a^{\lambda_2} + \beta_m^{\lambda_2}} = \frac{\mu R + (\mu - \psi)}{R}, \qquad (2)$$

where R is the scattering ratio at the wavelength of 353 nm; $\psi = \beta_{\lambda_1}^m / \beta_{\lambda_2}^m = (\lambda_2/\lambda_1)^4 = 1.725$; $\mu = \beta_{\lambda_1}^a / \beta_{\lambda_2}^a = (\lambda_2/\lambda_1)^\eta$ with the spectral dependence parameter η that, according to data of different authors, varies in the range $-2 < \eta < 2$.

The scattering ratio profiles, $R(h)$, in Eq. (2) are determined from the experimental data at the wavelength of 353 nm, parameter ψ is fixed, and the range of variation of μ is from $\mu(\lambda_1) = 0.76$ to $\mu(\lambda_2) = 1.31$ depending on the value of the parameter η. At $R = 6$ the value $\ln(\beta_{\lambda_1}^a / \beta_{\lambda_2}^a)(\mu_1) = -0.082$ and $\ln(\beta_{\lambda_1}^a / \beta_{\lambda_2}^a)(\mu_2) = 0.324$ that is comparable with the ozone optical thickness.

Before modeling the effect of the aerosol scattering on the accuracy of reconstruction of the ozone profile, let us pay attention to Eq. (1). We suggest to take into account the aerosol scattering in the form of integral values. In comparison with introducing the corrections through the extinction value,[15–16] the latter results in a more stable solution when reconstructing the ozone profiles.

CORRECTION FOR THE ABSORPTION TEMPERATURE DEPENDENCE

Temperature dependence of the ozone absorption coefficient in the Hartley and Huggins bands was revealed for the first time by E. Vigroux.[14] Investigations of the ozone absorption spectra, including refining the quantitative data with a simultaneous expansion of the wavelength and temperature ranges were continued in Refs. 17–23. Among the last investigations one should note Ref. 19, where measurements of the absolute values of the ozone absorption coefficients were carried out in the wavelength range 185–350 nm at temperatures 225–298 K. In spite of some difference in the quantitative results, one can note the intensification of the temperature dependence of the ozone absorption coefficient as the wavelength increases (from 300 to 350 nm). Then, according to Ref. 19, the ozone absorption coefficient at $\lambda = 350$ nm increases by 4 times in this temperature range, while that at $\lambda = 308$ nm increases only by 15%. Nevertheless, because of a small value of the absorption coefficient at $\lambda = 353$ nm ($\leq 0.3\%$ of the absorption coefficient at $\lambda = 308$ nm), the contribution into the differential absorption coefficient is negligible.

Figure 1 shows the data on the temperature dependence of the ozone absorption coefficient (according to the above cited papers) which are approximated by the square function of the form

$$K(T) = A + BT + CT^2 \ [\text{cm}^{-1} \cdot \text{atm}^{-1}], \qquad (3)$$

where $A = 1.32e + 0$; $B = 3.45e - 3$; $C = 2.12e - 5$; and T is temperature in °C.

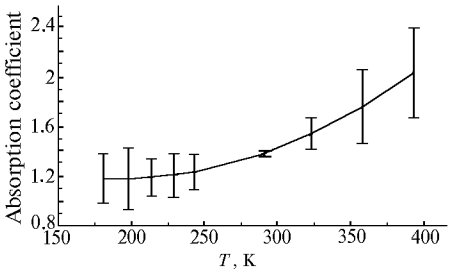

FIG. 1. Temperature dependence of the ozone absorption coefficient according to the literature cited in the paper.

It should be noted that the approximation results we obtained differ from the formulas obtained earlier.[24,25] The difference can be explained by the fact that we used newer and more correct data on the temperature dependence of the ozone absorption coefficient.

CORRECTION FOR THE ABSORPTION BY OTHER GASES

The absorption spectra of other gaseous components of the atmosphere are superposed on the UV absorption spectrum of the ozone molecules. First of all, in the wavelength range near 300–350 nm they are[3,15,16,26] SO_2 and NO_2.

The greatest values of the SO_2 absorption coefficient[3,14,27] are in the range near $\lambda = 300$ nm. The absorption spectra have the band structure with the spectral width of separate maxima (minima) of about 1 nm. The radiation at $\lambda = 308$ nm occurs in one of the absorption minima $K_{SO_2} = 4.87$ cm^{-1} ·atm^{-1}, and $K_{SO_2} = 0$ at $\lambda = 353$ nm. The contribution of SO_2 into the absorption can be revealed only in the troposphere, over strongly polluted areas, where the absorption at the ground level can reach the value[28] of 0.1 km^{-1}. When sensing in the altitude range 10–30 km the SO_2 concentration is more than two orders of magnitude less than that of O_3 at approximately the same absorption coefficients,[6,23] so even in the worst situation the neglect of the SO_2 absorption will not exceed 1% of the determined ozone concentration.

The NO_2 gaseous component has the absorption coefficient[29] of 4.6 cm^{-1} atm^{-1} at the wavelength of $\lambda = 308$ nm and 11.2 cm^{-1} atm^{-1} at $\lambda = 353$ nm. According to Ref. 30, the absorption over polluted areas can reach 0.15 km^{-1}. The maximum of NO_2 distribution in the stratosphere is at the altitudes of 25–30 km, and its content here is approximately two orders of magnitude less than the ozone content in its maximum.[3,31] This results in the differential absorption which is one order of magnitude less than the differential absorption by ozone even in the worst situation.

As to the effect of other small gaseous components such as mNO_3, m_2O_2, N_2O, N_2O_5 etc., according to the estimates[3,6] it is insignificant even in comparison with the total absorption by SO_2 and NO_2. Let us finally note that it is unlikely that the errors in determining the ozone profile related to neglecting the interfering gases can reach 2%, and in the case of taking them into account even from the model data can be reduced to a minimum.

THE RESULTS OF MODELING AND DATA PROCESSING

The account for aerosol and temperature stratification can be performed in several stages. At the first stage modeling and analysis of the stratifications of T and P were performed (separate, joint and their counter action). At the second stage the SOUND package[28,29] was updated, and at the third stage the package was directly used for processing real data of laser sensing.

The advantage of the approach we propose is in the possibility of calculating the temperature and aerosol stratifications from the same data with their subsequent account when reconstructing the ozone profile. This makes it possible to obtain more adequate data on the spatiotemporal ozone distribution.

Figure 2, where the results of numerical modeling of the account for the aerosol and temperature stratification at reconstruction of the ozone profiles are presented, confirms the aforesaid ideas. The modeled variations of the profiles of the scattering ratio and temperature relative to their mean values (5 and 10% of the maximum value) are shown in Fig. 2*a*. Figures 2*B–e* show the effect of neglecting the aerosol and temperature stratifications when reconstructing the ozone profile by Eq. (2). It is well seen that the neglect of the aerosol and temperature stratification results in a distortion of the reconstructed profile. One can see in Figs. 2*d* and *e* the intensification and compensation of the simultaneous effect of aerosol and temperature stratification on the reconstructed ozone profile. If the aerosol content in the atmosphere (formation of an aerosol layer) and temperature have increased, the neglect of these factors can result in an increase of the effect on the reconstruction of the ozone profile. And, vice versa, if the aerosol layer has appeared and temperature has decreased, there occurs compensation of the effect of neglecting these factors.

The aforementioned possibilities of taking into account the aerosol and temperature stratification are provided in a new version of the SOUND package. The block–diagram of the package is shown in Fig. 3. The new important addition is the possibility of calculating and taking into account the aerosol (by the scattering ratio) and temperature stratification. The techniques for reconstructing these parameters from the lidar return can be found in Refs. 31 and 32. Let us briefly describe the SOUND package operation.

1. The file with lidar return signals is selected and read.

2. The ozone profile is calculated automatically by adjusting coefficients (choice of the altitude, compression coefficient, etc.) which the user has set before.

3. It is suggested for the user to write the results of calculation (signals, optical thickness and ozone profile) into the output file, to continue the work with the selected signal (to change the adjusting coefficients, i.e. to change the altitudes, temperature models and scattering ratios, or to take the experimentally obtained ones, etc.), to start working with another signal (transition to the stage 1) or to finish the work.

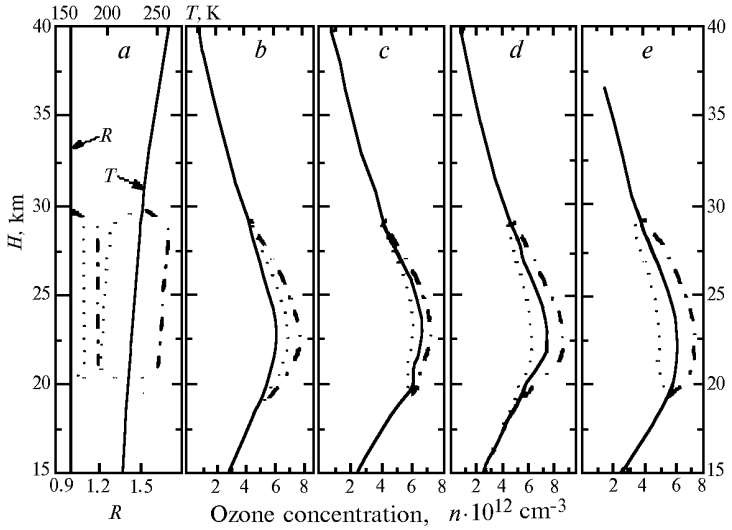

FIG. 2. Results of the numerical modeling of the account for aerosol and temperature stratification when reconstructing the ozone profiles; a) modeled variations of the scattering ratio and temperature profiles relative to the mean values (5 and 10% of the maximum value); b–e) effect of neglecting the aerosol and temperature stratification when reconstructing the ozone profile by Eq. (2).

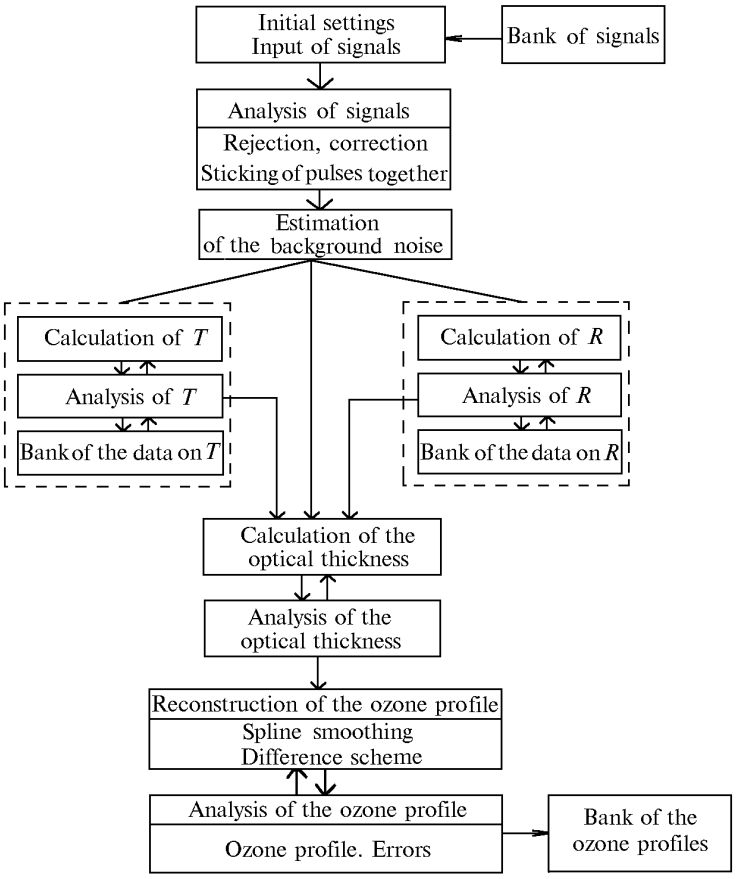

FIG. 3. Block–diagram of the SOUND software package.

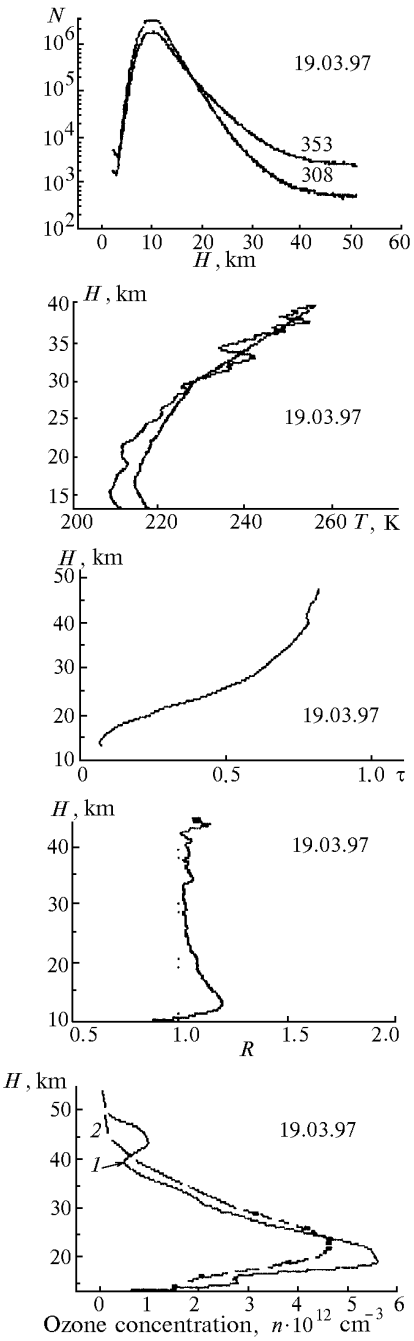

FIG. 4. Graphical data depicted by the package: lidar signals, temperature, optical thickness, scattering ratio and ozone profile (1) in comparison with the Kruger real profile (2).

The results of applying this package are shown in Fig. 4, where the data depicted by the package are presented (lidar signals, temperature, optical thickness, scattering ratio, and ozone profile). Figure 5 shows the effect of taking into account the aerosol and temperature stratification on the ozone profile reconstructed from the lidar data, and the profiles of temperature and the scattering ratios themselves. It is seen that the difference between the ozone profile reconstructed taking into account the scattering ratio (curve *4*), temperature (curve *3*), scattering ratio and temperature (curve *5*) and without the account for these parameters varies with the altitude and is the most sharp in the region of the ozone profile maximum (up to 30%) and at the altitude of 15 km (up to 40%).

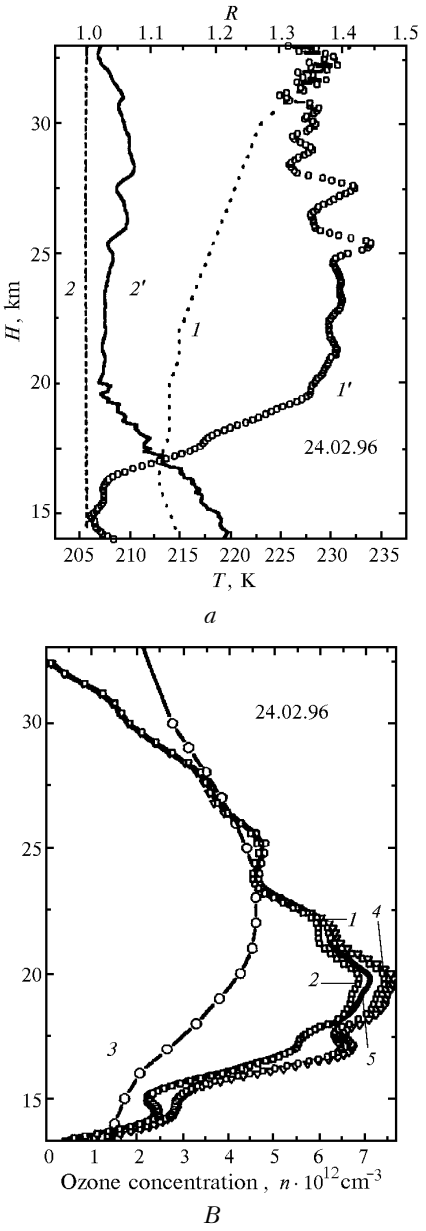

FIG. 5. The effect of taking into account the aerosol (1) and temperature (2) stratification on the ozone profile reconstructed from lidar data, in comparison with the Kruger model profile (3) and the profile obtained with both the account for stratification (4) and without the account for stratification (5) (b); modeling temperature (1), measurement temperature (1′) and modeling scattering ratio (2), measurement scattering ratio (2′) (a).

REFERENCES

1. P. McCormick, ed., *III Intern. Lidar Research Directory* (1993), 120 pp.
2. Network for detection of stratospheric change (NDSC) (1992).
3. G. Brasie and S. Solomon, *Aeronomy of the Middle Atmosphere* (Gidrometeoizdat, Leningrad, 1987), 367 pp.
4. O. Uchino, M. Maeda, and H. Hirono, J. Quant. Electr. **QE–15**, No. 10, 1094–1106 (1979).
5. O. Uchino, M. Maeda, et al., Appl. Phys. Lett. **33**, No. 9, 807–809 (1978).
6. V.M. Zakharov, O.K. Kostko, and S.S. Khmelevtsov, *Lidars and Investigation of Climate* (Gidrometeoizdat, Leningrad, 1996), 320 pp.
7. J.D. Klett, Appl. Opt. **20**, No. 2, 211–220 (1981).
8. J.D. Klett, Appl. Opt. **24**, No. 11, 1638–1643 (1985).
9. F.G. Fernard, Appl. Opt. **23**, No. 5, 652–653 (1984).
10. A. Papayanis, G. Ancellet, et al., Appl. Opt. **29**, No. 4, 467–476 (1990).
11. E.V. Browell, S. Ismail, et al., Appl. Opt. **24**, No. 17, 2827–2836 (1985).
12. V.D. Burlakov, A.V. El'nikov, V.N. Marichev, V.V. Zuev, et al., Atmos. Oceanic Opt., No. 10, 1224–1233 (1993)
13. V.E. Zuev and G.M. Krekov, *Optical Models of the Atmosphere* (Gidrometeoizdat, Leningrad, 1986), 256 pp.
14. E. Vigroux, Ann. Paris **8**, 709 (1953).
15. E.C. Inn and Y. Tanaka, J. Opt. Soc. Am. **43**, 870–872 (1963).
16. M. Griggs, J. Chem. Phys. **49**, 857–859 (1968).
17. R.D. McPeters and A.M. Bass, Geophys. Res. Lett. **49**, No. 3, 227–230 (1982).
18. J.W. Simons, J. Chem. Phys. **59**, No. 3, 1203–1208 (1973).
19. L.T. Molina and M.T. Molina, J. Geophys. Research **91**, No. D13, 14501–14508 (1988).
20. R.M. Measures, *Laser Remote Sensing* (John Wiley and Sons, New York, 1987).
21. E.D. Hinkly, ed., *Laser Monitoring of the Atmosphere* (Springer Verlag, New York, 1976).
22. O.K. Kostko, et al., *Application of Lasers to Deternining Composition of the Atmosphere* (Gidrometeoizdat, Leningrad, 1983), 226 pp.
23. D.B. Merzon, Probl. Fiz. Atmos., No. 18, 42–63 (1986).
24. V.N. Marichev and A.V. El'nikov, Opt. Atm., No. 5, 77–78 (1988).
25. O.J. Brassington, Appl. Opt. **20**, No. 21, 3774–3778 (1981).
26. G. Megie, Appl. Opt. **24**, No. 21, 3455–3463 (1988).
27. I.I. Ippolitov, V.S. Komarov, and A.A. Mitsel, in: *Spectroscopic Methods for Sensing of the Atmosphere* (Nauka, Novosibirsk, 1985), pp. 4–14.
28. V.V. Zuev, V.N. Marichev, M.Yu. Kataev, and A.A. Mitsel, Dep. VINITI, No. 4690–94 (1994), 32 pp.
29. V.V. Zuev, V.N. Marichev, M.Yu. Kataev and A.A. Mitsel, in: *Abstracts of papers at II Interrepublic Symposium "Atmospheric and Oceanic Optics"*, Part 2, (1995), pp. 270–271.
30. V.V. Zuev and V.S. Komarov, *Gaseous Components of the Atmosphere* (Gidrometeoizdat, Leningrad, 1986), 295 pp.
31. V.V. Zuev, V.N. Marichev, et al., Atmos. Oceanic Opt. **9**, No. 10, 875–878 (1996).
32. A.V. El'nikov, V.V. Zuev, M.Yu. Kataev, and V.N. Marichev, Atmos. Oceanic Opt. **4**, No. 2, 175–182 (1991).
33. A.V. El'nikov, V.V. Zuev, M.Yu. Kataev, V.N. Marichev, et al., Atmos. Oceanic Opt. **5**, No. 6, 362–369 (1992).